

MEASUREMENTS OF THE FEL-BANDWIDTH SCALING WITH HARMONIC NUMBER IN A HGHG FEL *

Enrico Allaria[#], Miltcho B. Danailov, William M. Fawley,
Elettra-Sincrotrone Trieste S.C.p.A., Basovizza, Italy

Luca Giannessi,

Elettra-Sincrotrone Trieste S.C.p.A., Basovizza, Italy and ENEA C.R. Frascati, Frascati (Roma), Italy

Eugenio Ferrari,

Elettra-Sincrotrone Trieste S.C.p.A., Basovizza, Italy and Università degli Studi di Trieste, Trieste, Italy

Abstract

In this work we report recent measurements done at FERMI showing the dependence of the FEL bandwidth with respect to the seed laser harmonic at which the FEL is operated. Comparison of FEL spectra for different Fourier-limit seed and chirp pulses is also reported.

THE HGHG FEL AT FERMI

FERMI is the seeded FEL system in operation at Trieste and running for user's experiment that can use high power pulses in the VUV – soft X-ray spectral range characterized by a high degree of coherence [1,2] and also variable polarization [3]. The two FELs, in operation at FERMI, in order to cover the spectral range that goes from 100 nm down to 4 nm are based on the high gain harmonic generation scheme [4]; this uses an external laser in the UV to initiate the coherent emission at his harmonics that is then amplified by the FEL process. Since the external coherent seed imposes an exact phase relation between various electrons participating to the FEL emission, the seeding is crucial for improving the longitudinal coherence. However, it has been pointed out that the method is affected, like other frequency multiplication processes, by the phase noise amplification [5]. As a consequence of the harmonic conversion, a small residual phase noise in the seeding signal could significantly deteriorate the phase of FEL radiation up to the point to destroy the longitudinal coherence.

Recently a series of numerical simulation have been done for a simplified HGHG FEL showing that as a consequence of the nonlinear process of the bunching creation the time-bandwidth product deterioration due to residual chirp in the seed laser is partially mitigated [6].

By measuring the dependency of the FEL bandwidth as a function of the FEL harmonic and of the seed laser residual chirp, we experimentally investigate the phase noise amplification process in a seeded FEL.

The Seed Laser

Since the FEL process is initiated by the seed laser and the properties of the FEL depend on the quality of the laser a lot of effort has been dedicated at FERMI to guarantee a high performance of the seed laser system, a detailed description can be found in [7]. Depending on the

need of the FERMI user to have complete tunability of the FEL or not the seed pulses can be obtained either by using the third harmonic of a Ti:Sapphire laser (THG), or by the use of an Infrared Optical Parametric Amplifier (OPA) with consequent frequency up-conversion to UV. Main parameters for the two possible configurations are reported in Table 1 and Table 2.

Table 1: Seed Laser Parameters for the THG

Parameter	
Pulse length (FWHM)	120 fs
Bandwidth (FWHM)	~0.8 nm
Central Wavelength	261 nm ±1 nm
Energy per pulse	10-100 μJ

It should be noted that in the case of THG seeding the available UV pulse energy allows to use a grating compressor and compensate the linear chirp introduced by the rather complex beam-transport. However, in the case of OPA seeding at present the seed pulses cannot be compressed and contain a residual positive chirp.

Table 2: Seed Laser Parameters for the OPA in the Most Frequently Used 230-262 nm Seed Wavelength Range

Parameter	
Pulse length (FWHM)	120-150 fs
Bandwidth (FWHM)	1-1.1 nm
Central Wavelength	230-262 nm
Energy per pulse	7-50 μJ

The Electron Beam

Because electrons are the medium used in the FEL amplification, it is clear that the quality of the electron beam is another crucial parameter. In particular it has been shown how possible modulation in the longitudinal phase space can deteriorate the FEL bandwidth. For this reason the typical electron beam used for normal operations at FERMI has a moderate compression and a lot of effort is done in order to linearize the longitudinal phase space [8] and suppress the microbunching [9].

*Work partially supported by the Italian Ministry of University and Research under grants FIRB-RBAP045JF2 and FIRB-RBAP06AWK3
#enrico.allaria@elettra.eu

The electron beam parameters used during these measurements are reported in Table 3.

Table 3: Electron Beam Parameters

Parameter	
Peak current (A)	~500
Charge (pC)	500
Energy (GeV)	1.2
Energy spread (keV)	150
Emittance (mm mrad)	1
Beam size (mm)	0.15

MEASUREMENTS

For this experiment the FEL has been characterized looking at the spectra that can be acquired with the available diagnostic at FERMI [10]. FEL spectra are measured acquiring the images of the energy dispersed FEL radiation on a YAG. The acquisition done through the FERMI control system allows one to acquire either the full CCD image or only the signal projected along the wavelength axis. In this work, we mainly acquired the simple projections but in few cases the full images have been acquired, like the case showed in Fig. 1.

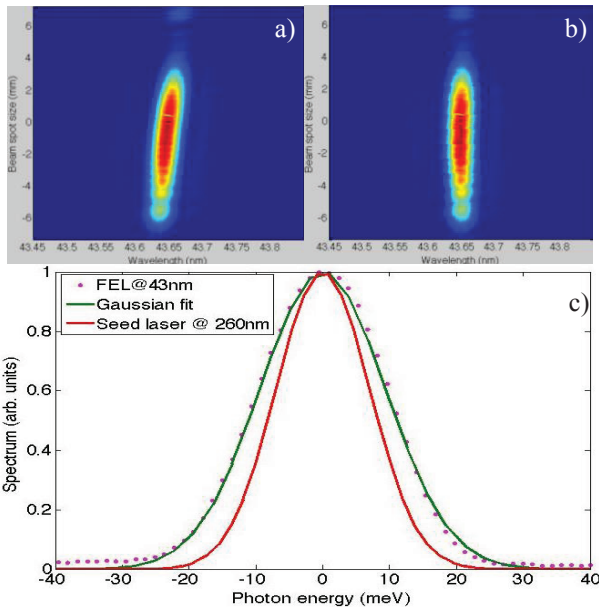


Figure 1: a) direct image of the acquired FEL spectra at 43 nm; b) a numerical correction is applied in order to remove the small residual tilt due to the CCD. c) The projection of the image along the horizontal axis is used to obtain the FEL spectrum to be compared to the seed laser spectrum.

For each studied configuration we acquired long sequences of spectra that has been statistically analysed and whose typical distribution for the FEL bandwidth is

reported in Fig. 2 showing the case of 43 nm obtained with the THG seed laser.

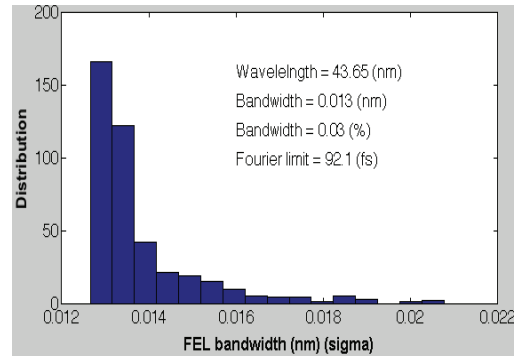


Figure 2: Distribution of the FEL bandwidth at 43 nm.

The data present an asymmetric distribution with a peak toward narrow bandwidth and a long tail to large bandwidths. Such a distribution can be explained taking into account that the timing jitter between the electron beam and the seed laser can occasionally place the seed laser far from the good region where the phase space distortions of the electron beam deteriorate the FEL spectra. This fact is confirmed by looking at the correlation between the FEL spectra and the compression signal that is known to be related to the electron beam arrival time (Figure 3).

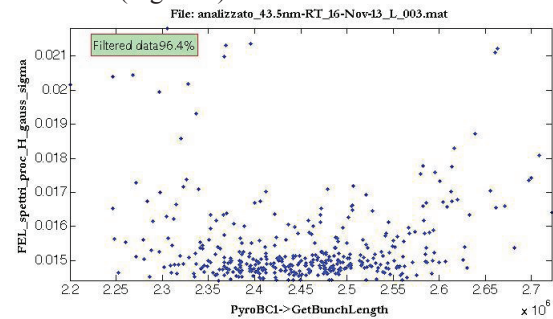


Figure 3: Correlation curve between the FEL spectrum and the electron beam compression signal.

Given that the tail in the distribution is coming from the electron beam properties, in order to characterize the impact of the seed on the FEL spectra and his dependence with the harmonic number we discard those shots characterized by a too large bandwidth.

Using the same seed laser and the same electron beam scan of the FEL wavelength from 23 to 62 has been done changing the FEL harmonic from the 4th to the 11th. For every FEL wavelength in addition to change the undulator resonance, the seeding power and the strength of the dispersive section where slightly optimized.

In figure 4 the evolution of the FEL bandwidth as a function of the FEL harmonic is shown both in absolute and relative scale (Fig. 4-a, b). In order to take into account the small contribution to the bandwidth coming from the CCD tilt, when possible the bandwidth has been measured from the rotated images as in Fig. 1b. When this was not possible we apply a similar correction to the bandwidth obtained from the non-corrected images.

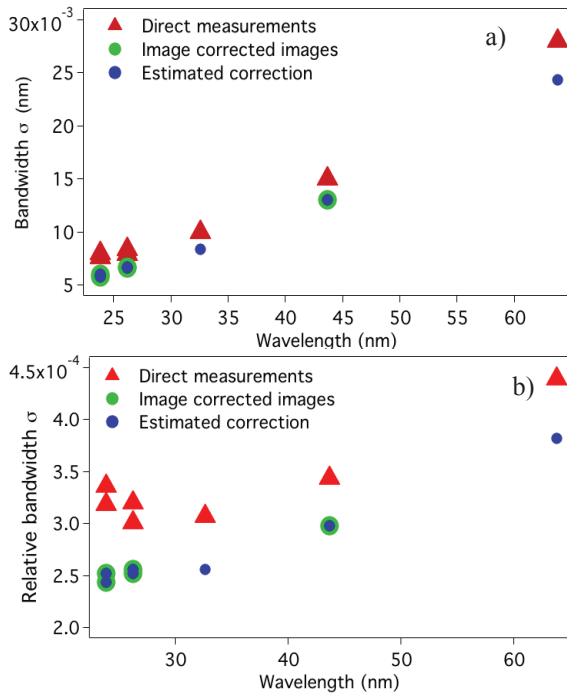


Figure 4: Measured FEL bandwidth for different harmonics in nm (a) and normalized to the FEL wavelength (b).

The FEL Pulse Shortening

Because the measured spectra are well fitted by a Gaussian curve we can estimate the FEL pulse length from the spectrum with the equation:

$$\Delta t_{FWHM} = \frac{0.44}{\Delta \omega_{FWHM}}. \quad (1)$$

This easy calculation for the FEL pulse length makes the strong assumption that FEL pulses are fully coherent and no chirp or phase noise is present. Given the already mentioned phase noise amplification, such a hypothesis is expected to be less valid as we go toward shorter wavelength (higher harmonics). But in any case this approximation allow to calculate the lower limit for the pulse lengths at various harmonics, indeed shorter pulses would necessarily imply a bandwidth larger than the one measured.

Using the data for the FEL bandwidth reported in Figure 4 with Eq. (1) we obtain the expected evolution of the pulse length as a function of the wavelength and harmonic (Figure 5).

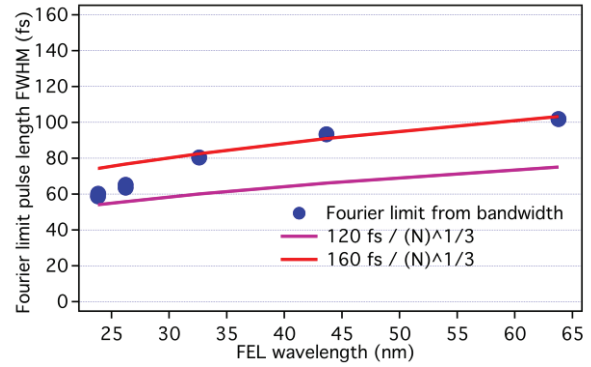


Figure 5: Calculated pulse length from the measured spectral bandwidth (blue dots) and estimated pulse length assuming the scaling law with the harmonic described by Eq. (2) [6].

The calculated pulse length can be compared with the one that can be calculated according to the theory presented in [6] that predict scaling law for the FEL pulse with respect to the harmonic that can be described by:

$$\Delta t^{FEL} = \frac{\Delta t^{seed}}{\sqrt[3]{N_H}}. \quad (2)$$

where, Δt^{seed} , is the pulse length of the seed laser, and N_H is the harmonic at which the FEL is operated.

Equation (2) is used with the nominal seed laser pulse length (120 fs) for the magenta curve in Figure 5, in addition a curve for a seed laser of 160 fs has been also plotted.

Because our measurements set the lower limit for the real FEL pulse length we see that the data can not be fitted with the pulse shortening scaling law predicted in [6] if one consider the seed laser pulse length that has been measured in the laser table (taking into account the effects for all the optics driving the laser into the FEL). Experimental measurements and theoretical prediction would better fit if one considers a seed laser 160 fs long (red curve in Figure 5). In this case there is a good agreement for the longer wavelengths (lower harmonics) where we expect the bandwidth degradation due to the phase noise multiplication to be limited. A virtual shortening (due to a bandwidth enlargement) of the points at shorter wavelengths could be the results of a reduced longitudinal coherence and an increase of the phase noise for this high harmonic cases.

FEL Bandwidth Degradation due to Seed Pulse Residual Phase Curvature

A second experiment has been done by changing the seeding properties while keeping other parameters (FEL wavelength, harmonic, electron beam) constant. We note that when OPA is used for seeding, the pulses arriving in the undulator have a non-negligible residual phase curvature (both linear and higher order terms). The non-flat phase comes from the OPA scheme (which involves chirped white light continuum for the OPA seeding), the frequency up-conversion to UV where GVM effects are

non-negligible, and from the beam transport optics containing a number of reflections on broadband UV multilayer mirrors as well as propagation in about 12 mm of fused silica. In the case of THG seeding, the linear chirp (i.e. second order phase) caused by the beam transport can be pre-compensated by the use of a dedicated UV grating compressor.

To understand the influence of this difference on the generated FEL light quality we compare the FEL spectra at 23 nm (11th harmonic) generated first with seeding in THG mode and then in OPA mode where both were set at about the same wavelength (262 nm) and had bandwidths of 0.8 and 1 nm, respectively. As it can be seen from the cross-correlation traces shown on Fig. 6, the OPA pulse is longer and has nearly two times higher time-bandwidth product due to an estimated uncompensated GDD of about $2.5 \times 10^3 \text{ fs}^2$.

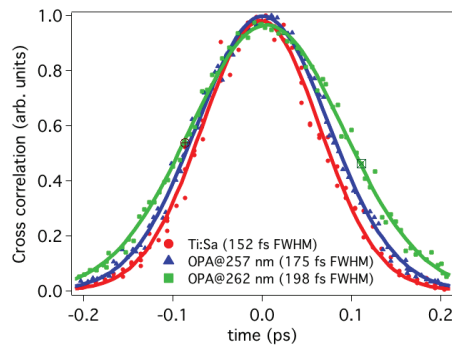


Figure 6: Cross correlation curves of the seed laser in the THG and OPA configurations.

The effect of the seed laser chirp has been measured looking at relatively short wavelengths (high harmonics) where the effect is expected to be stronger.

Figure 7 shows a comparison between what is measured using the THG seed laser and the OPA at 262 nm.

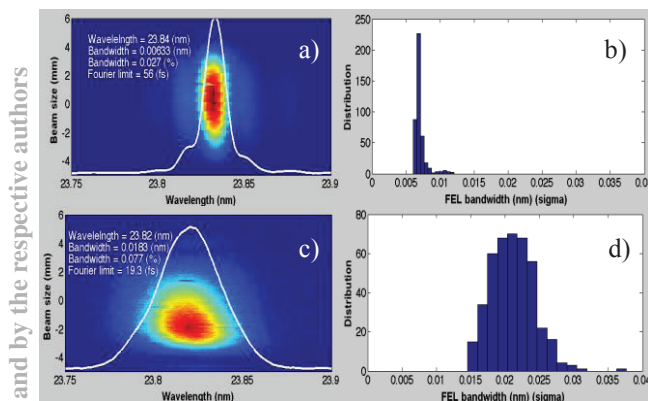


Figure 7: FEL spectrum and his distribution for the FEL at 23 nm using the THG (a,b) and the OPA (c,d) as a seed.

Our results show that when operating at relatively high harmonics ($N_H = 11$) a small change in the seed laser coherence properties has a strong impact in the FEL pulse length and bandwidth as expected from the phase noise frequency multiplications.

CONCLUSION

In the reported measurements we have shown the bandwidth properties of the FEL in seeded HGHG configuration both as a function of the FEL harmonic and of the seed laser quality. The influence of the seed laser pulse phase distortions on the FEL spectrum quality is significant at high harmonic and may spoil the seeding benefits at very short wavelength. It is therefore planned to dedicate an additional effort (e.g. by implementing an adaptive seed pulse shaping) for providing a better control on the UV pulse quality in both THG and OPA mode. Moreover further FEL studies combining spectral properties to FEL pulse length would give more information about the effective pulse shortening and bandwidth degradation occurring in the harmonic generation.

ACKNOWLEDGMENT

We are pleased to acknowledge the extensive assistance we have received from the FERMI commissioning and the laser teams during the operation of the FEL during the dedicated measurements.

REFERENCES

- [1] E. Allaria *et al.*, Nat. Photon. **6**, 699 (2012).
- [2] E. Allaria *et al.*, Nat. Photon. **7**, 913 (2013).
- [3] E. Allaria *et al.*, submit.
- [4] L.H. Yu, Phys. Rev. A **44**, 5178–5193 (1991).
- [5] E.L. Saldin *et al.*, Opt. Commun. **281**, 1179–1188 (2008).
- [6] D. Ratner *et al.*, Phys. Rev. ST Accel. Beams **15**, 030702 (2012).
- [7] M.B. Danailov *et al.*, Proceedings of FEL conference 2011, TUOC4, Shanghai (China) 2011.
- [8] G. Penco *et al.*, FEL conference 2013, TUOCNO01, New York (USA) 2013.
- [9] S. Spampinati *et al.* in preparation.
- [10] M. Zangrando *et al.*, Rev. Sci. Instrum. **80**, 113110 (2009).